Cyclic AMP-dependent plasticity underlies rapid changes in odor coding associated with reward learning

Thierry Louis[a], Aaron Stahl[a], Tamara Boto[a], and Seth M. Tomchik[a,1]

[a]Department of Neuroscience, The Scripps Research Institute, Jupiter, FL 33458

Edited by Mani Ramaswami, Trinity College Dublin, Dublin, Ireland, and accepted by Editorial Board Member John R. Carlson December 4, 2017 (received for review May 31, 2017)

Learning and memory rely on dopamine and downstream cAMP-dependent plasticity across diverse organisms. Despite the central role of cAMP signaling, it is not known how cAMP-dependent plasticity drives coherent changes in neuronal physiology that encode the memory trace, or engram. In *Drosophila*, the mushroom body (MB) is critically involved in olfactory classical conditioning, and cAMP signaling molecules are necessary and sufficient for normal memory in intrinsic MB neurons. To evaluate the role of cAMP-dependent plasticity in learning, we examined how cAMP manipulations and olfactory classical conditioning modulate olfactory responses in the MB with in vivo imaging. Elevating cAMP pharmacologically or optogenetically produced plasticity in MB neurons, altering their responses to odorants. Odor-evoked Ca^{2+} responses showed net facilitation across anatomical regions. At the single-cell level, neurons exhibited heterogeneous responses to cAMP elevation, suggesting that cAMP drives plasticity to discrete subsets of MB neurons. Olfactory appetitive conditioning enhanced MB odor responses, mimicking the cAMP-dependent plasticity in directionality and magnitude. Elevating cAMP to equivalent levels as appetitive conditioning also produced plasticity, suggesting that the cAMP generated during conditioning affects odor-evoked responses in the MB. Finally, we found that this plasticity was dependent on the Rutabaga type I adenylyl cyclase, linking cAMP-dependent plasticity to behavioral modification. Overall, these data demonstrate that learning produces robust cAMP-dependent plasticity in intrinsic MB neurons, which is biased toward naturalistic reward learning. This suggests that cAMP signaling may serve to modulate intrinsic MB responses toward salient stimuli.

learning | memory | cAMP | plasticity | imaging

Learning generates plasticity in neuronal responses to input stimuli, which is distributed across multiple cells and synapses in the brain. Molecularly, dopamine and downstream cAMP signaling are involved in multiple forms of memory, including olfactory learning. For instance, dopamine is required in the amygdala for olfactory classical conditioning in mammals (1). Similarly, dopamine and downstream cAMP signaling molecules play a central role in olfactory classical conditioning in *Drosophila*. This pathway is particularly critical in the mushroom body (MB), a brain region that receives olfactory information and is required for olfactory learning. Dopaminergic neurons are postulated to convey a reinforcement signal to the MB—stimulating certain subsets of MB-innervating dopaminergic neurons drives aversive or appetitive reinforcement in lieu of a physical reinforcer (2–5). The dopamine released from these neurons acts directly on intrinsic MB neurons, and possibly other neurons in the area as well (6–11). The D1-like receptor DopR, type I adenylyl cyclase Rutabaga (Rut), catalytic domain of protein kinase A, and Dunce phosphodiesterase (Dnc) are all required for olfactory classical conditioning. Importantly, rescuing the expression of DopR or Rut—specifically in intrinsic MB neurons of otherwise mutant animals—restores normal olfactory learning and memory (7, 10, 12–18). Further downstream, both Epac and PKA, as well as phosphorylation targets such as synapsin, have been shown to regulate learning and memory via effects in MB neurons (19–23). Thus, dopamine and cAMP are critical in intrinsic MB neurons for normal memory. Furthermore, broadly elevating cAMP generates plasticity in MB neurons, demonstrating that this pathway influences the responsivity of MB neurons (8, 24). However, the role of this pathway in driving coherent patterns of plasticity that encode memory is unknown.

Recent advances have opened up the possibility of understanding how olfactory memory is encoded in exquisite detail (25). Recent studies of memory encoding in the *Drosophila* MB have suggested that mushroom body neurons are highly plastic, exhibiting learning-related changes in odor responses. This is supported by observations of memory traces using in vivo Ca^{2+} imaging of neurons innervating the MB (26–33). However, the neuronal changes associated with cAMP-dependent, short-term memory are unclear. Conditioning generates plasticity in α′/β′-neurons within a few minutes of training (33, 34), a time point at which the animals exhibit robust short-term memory. However, the Rut cyclase is not required in α′/β′-neurons for learning (17), leaving the functional role of cAMP-dependent plasticity in the MB unclear. MB γ-neurons exhibit depression in response to an aversive conditioned odor that is sensitive to manipulations of Gαo-signaling (35), though it is not clear how this relates to dopaminergic modulation via Gαs. Finally, blocking the synaptic output of MB neurons during conditioning does not impair aversive learning, suggesting that a significant proportion of the engram resides in the MB neurons and/or upstream connections (36–38) (though see ref. 6).

In contrast, other studies have described a major role for plasticity in downstream MB output neurons (MBONs), which may arise via pre- and/or postsynaptic plasticity. Robust, dopamine-dependent plasticity has been observed in MBONs, but not at the cellular level in MB neurons (11, 39–41). This emphasizes the role of the MB in encoding sparse, relatively invariant olfactory representations (42, 43). Learning-induced plasticity is then layered in at the MB–MBON

Significance

Cyclic AMP signaling is involved in learning across taxa, but how cAMP modulation drives coherent plasticity across circuits is unclear. Results of this study demonstrate that cAMP-dependent plasticity in the *Drosophila* brain drives olfactory learning-induced plasticity, which is biased toward appetitive conditioning and modulates motivated behavior.

Author contributions: T.L. and S.M.T. designed research; T.L., A.S., and T.B. performed research; T.L. contributed new reagents/analytic tools; T.L., A.S., T.B., and S.M.T. analyzed data; and T.L. and S.M.T. wrote the paper.

The authors declare no conflict of interest.

This article is a PNAS Direct Submission. M.R. is a guest editor invited by the Editorial Board.

[1]To whom correspondence should be addressed. Email: stomchik@scripps.edu.

This article contains supporting information online at www.pnas.org/lookup/suppl/doi:10.1073/pnas.1709037115/-/DCSupplemental.

synapses, possibly via synaptic depression (11, 40, 44, 45). This leaves the requirement of cAMP signaling molecules in the MB, and the dispensability of MB output during memory acquisition, unresolved. Thus, there is a paradoxical dissociation of anatomical loci between where cAMP signaling is required and where robust, short-term, learning-induced plasticity has been reported. Here we have examined the role of cAMP-dependent plasticity in the MB using in vivo imaging, combined with pharmacological and optogenetic manipulation of cAMP levels. Results suggest that cAMP-dependent plasticity localizes to intrinsic MB neurons and mirrors the plasticity induced during olfactory classical conditioning, with a bias toward appetitive conditioning.

Results

Elevation of cAMP Drives Plasticity in Mushroom Body Neurons. To examine the localization of cAMP-dependent plasticity, we imaged odor-evoked Ca^{2+} responses in the MB before and after elevating cAMP transiently (Fig. 1*A*). The MB contains three major anatomical classes of neurons: α/β, α′/β′, and γ, named according to the lobes that their axons innervate (α, α′, β, β′, and γ) (Fig. 1*B*) (46). Some of these can be further subdivided by anatomical criteria: α/β [core (outer and inner), shell, posterior] and α′/β′ (anterior, middle, posterior) (γ-neurons are more homogeneous) (47, 48). The genetically encoded Ca^{2+} indicator UAS-GCaMP6f was expressed in different major subsets of MB neurons with subset-selective Gal4 drivers. Each of the MB lobes can be subdivided into two to five subdomains based on anatomical criteria (γ1 to γ5, α1 to α3, β1 and β2, α′1 to α′3, β′1 and β′2) (49). For most analyses, the γ2–5-subdomains were pooled into a single anatomically contiguous region of interest (ROI), as were the β1- and β2-subdomains (Fig. 1*C*). Odor-evoked Ca^{2+} responses were imaged before and after pairing the odor with pharmacological elevation of cAMP via transient forskolin application (Fig. 1 *D*–*F*). In initial experiments, GCaMP6f was expressed broadly in the MB with the R13F02-Gal4 (50) or 238Y driver, and odor responses were imaged in the MB α-, β-, and γ-lobes. Both γ1- and γ2–5-ROIs were significantly elevated relative to controls (Fig. 1 *E*–*G*). When the γ2–5-regions were parsed and analyzed independently, the effect was significant in γ1 and γ5, with a trend in the same direction across the other regions (Fig. S1). In α/β-neurons, an increase was observed in the α-, but not β-, lobe (Fig. 1 *F* and *H*). This could result from either a differential effect across these lobes or from relatively weak plasticity that exceeds the detection threshold only under certain experimental conditions. Therefore, we further examined the localization of cAMP-dependent plasticity, driving GCaMP with MB subset-selective Gal4 drivers: γ (R64C08 and 1471) and α/β (R34B09). Across all γ-drivers, both the γ1- and γ2–5-ROIs revealed significantly higher responses following cAMP elevation than in saline controls (Fig. 1 *E*–*G*). In contrast, the α- and β-lobes exhibited enhancement in some drivers/ROIs but not others (Fig. 1*H*).

The mixed results in α/β-neurons with different drivers/ROIs suggest that plasticity may be present in these neurons, though it

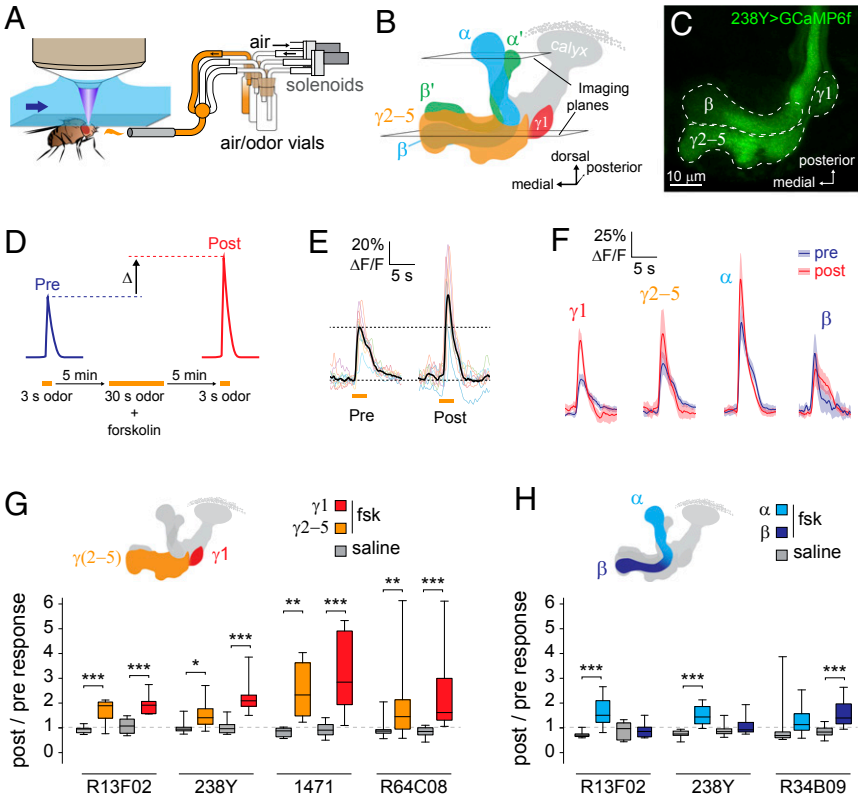

Fig. 1. Elevating cAMP increased the magnitude of odor-evoked Ca^{2+} transients in the MB. (*A*) Drawing of the in vivo imaging preparation. (*B*) Drawing of a frontal view of the MB, with the lobes of α/β-, α′/β′-, and γ-neurons indicated with different colors. (*C*) Confocal image of GCaMP6f expressed using the broad MB driver 238Y-Gal4. (*D*) Experimental protocol. (*E*) Pre- and postforskolin odor-evoked responses, imaged from the MB γ-lobe (γ2 to γ5) in R13F02-Gal4>UAS-GCaMP6f flies. Responses from individual flies are plotted as thin lines, and the mean response is represented by the thick black line. Odor presentation time is indicated with the orange bar. (*F*) Pre- and postpairing odor responses (mean ± SEM), imaged from different ROIs in R13F02-Gal4>UAS-GCaMP6f flies. (*G*) Change in odor responses following forskolin or saline (controls) in MB γ-neurons, using R13F02 (n = 10/12 for saline/forskolin), 238Y (n = 15/15), 1471 (n = 12/12), and R64C08 (n = 12/16) Gal4 drivers. $^{*}P < 0.05$, $^{**}P < 0.01$, $^{***}P < 0.001$ (Sidak). Fsk, forskolin. (*H*) Change in odor responses following pairing of odor with forskolin or saline in MB α/β-neurons, using R13F02 (α n = 11/11 for saline/forskolin; β n = 12/11), 238Y (α n = 12/12; β n = 15/15), and R34B09 Gal4 (α n = 12/12; β n = 12/12) drivers. $^{***}P < 0.001$ (Sidak).

falls below the detection threshold under some experimental conditions. Therefore, to probe the effects of cAMP on MB subsets with higher sensitivity, we turned to the presynaptically tethered reporter synaptophysin-GCaMP3 (syp-GCaMP3) (51, 52). This enhances the sensitivity of the reporter and biases it toward neurotransmitter release-coupled synaptic Ca^{2+} transients (53). As above, a panel of MB drivers was tested. With the relatively broad 238Y-Gal4 driver, we observed cAMP-dependent enhancement across multiple MB regions, including the α- and β-lobes (Fig. S2 *B* and *C*). Significant increases in odor-evoked responses were also observed in the γ1- and γ2–5-regions with the γ-selective R64C08-Gal4 driver (Fig. S2*C*), and in the α-lobe with the α/β-specific driver R34B09 (Fig. S2 *B* and *C*) (β-lobe fluorescence was too weak to image with this driver/reporter combination). Thus, synaptically tethered GCaMP revealed plasticity in two cases where it was not significantly elevated with cytosolic reporters (Fig. 1*H* and Fig. S2 *B* and *C*). Overall, these data suggest that elevating cAMP produced strong increases in odor-evoked responses in MB γ-lobes, with smaller and/or more localized synaptic plasticity in α/β-neurons.

Plasticity Is Intrinsic to Mushroom Body Neurons. Olfactory information flows from olfactory receptor neurons in the periphery through second-order projection neurons in the antennal lobes to the third-order MB neurons. Therefore, increases in MB neuron responses to odorants could result from changes in either the MB neurons themselves or the upstream projection neurons that provide their olfactory input. To test this, we separately imaged projection neurons and MB neurons in the calyx, where the MB neurons receive input from projection neurons. GCaMP was expressed in either the olfactory projection neurons or the MB neurons, and the effect of forskolin on odor-evoked Ca^{2+} responses was examined. Three GCaMP variants were used: cytosolic GCaMP6f, presynaptically tethered syp-GCaMP3, or postsynaptically tethered homer-GCaMP3 (51). This allowed direct comparison of the cAMP-dependent plasticity on both sides of the synapse between projection neurons and MB neurons. Information flow in the calyx is bidirectional, with both projection neurons and MB neurons having pre- and postsynaptic elements in the calyx (54–56). Therefore, we expressed each GCaMP variant in each neuron class and imaged the calyx, analyzing all six combinations in separate experiments (Fig. 2 *A*–*C* and Fig. S3). With all three reporters, MB neurons showed a significant increase in postforskolin odor responses relative to saline controls (Fig. 2*D*). In contrast, projection neurons showed a significant decrease with cytosolic and syp-GCaMP, and no change with homer-GCaMP (Fig. 2*D*). Thus, the cAMP-induced increases in MB odor responses cannot be attributed to facilitation in the upstream olfactory pathway.

Intrinsic MB neurons are interconnected with a variety of extrinsic neurons (29, 47, 49, 57, 58). Therefore, pharmacological cAMP manipulation could generate plasticity via actions on these other interconnected components of the circuit. To localize elevation of cAMP to intrinsic MB neurons, we implemented an optogenetic approach. The photoactivatable adenylyl cyclase bPAC (59) was coexpressed with the red-shifted, genetically encoded Ca^{2+} reporter R-GECO (60) in the MB. This combination allowed discrete optogenetic elevation of cAMP and imaging of odor-evoked responses. Odor responses were imaged in the β- and γ-lobes before and after pairing odor with stimulation of bPAC via blue light (Fig. 3 *A* and *B*). In the γ1- and γ2–5-regions, odor responses were facilitated in bPAC-expressing flies relative to controls lacking the cyclase (Fig. 3*C*). While there was a trend in the β-lobe, the difference was not statistically significant. There was no difference in odor-evoked responses in control experiments where animals were not exposed to blue light (Fig. 3*C*). While bPAC does not generate detectable cAMP in the absence of light stimulation (59), ectopic expression could

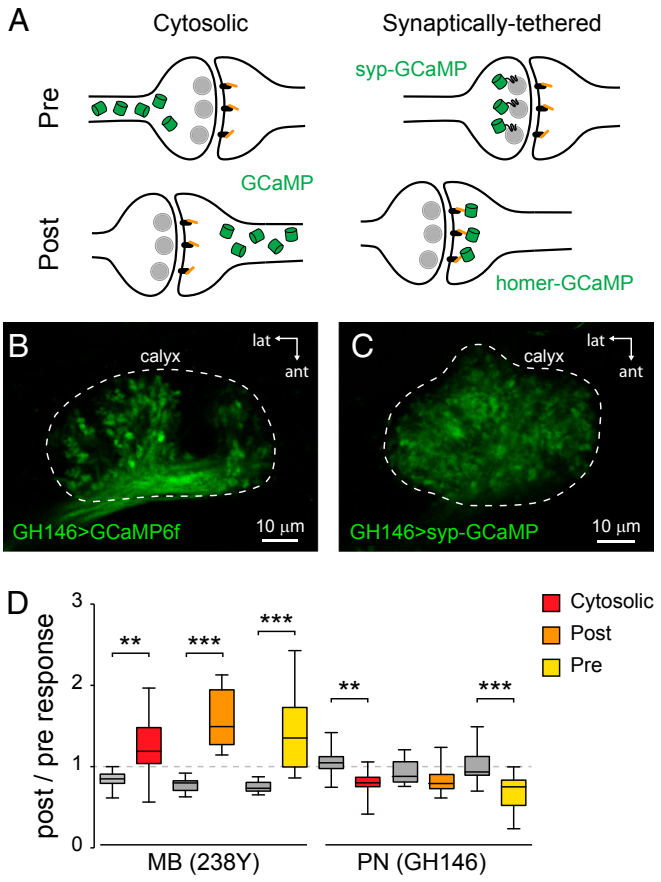

Fig. 2. Plasticity in odor-evoked Ca^{2+} responses is not attributable to upstream olfactory projection neurons. (*A*) Drawing of the subcellular and pre/postsynaptic localization of GCaMP variants at the projection neuron (PN)–MB synapse: cytosolic (UAS-GCaMP6f), presynaptically tethered (syp-GCaMP3), or postsynaptically tethered (homer-GCaMP3). (*B*) Expression of cytosolic GCaMP in PNs, imaged in the calyx, where PNs synapse with MB neurons (unlabeled). GCaMP was expressed with the PN-specific driver GH146-Gal4. (*C*) Presynaptically tethered syp-GCaMP3 expression in PNs, imaged in the calyx. Note the specific localization of GCaMP in the synaptic terminals and its absence in the axonal shafts. (*D*) Box plots showing the change in odor-evoked Ca^{2+} responses following pharmacological elevation of cAMP with forskolin ($n > 12$ per group). Because information flow in the calyx is bidirectional, all three GCaMP variants were expressed both in the MB neurons (238Y) and PNs (GH146), and the calyx was imaged with all six combinations. Ethyl butyrate was presented as the odorant. $^{**}P < 0.01$, $^{***}P < 0.001$ (Sidak).

conceivably alter neuronal function. To test this possibility, we expressed bPAC in the MB using the same 238Y-Gal4 driver as above, and tested olfactory aversive conditioning, which relies on intact MB function (36, 37). In this behavioral assay, bPAC-expressing flies exhibited no impairment of olfactory learning relative to the two controls (Fig. 3*D*) ($P = 0.10$, ANOVA). Overall, these data suggest that elevating cAMP enhances odor-evoked responses specifically via actions in the intrinsic MB neurons.

Elevation of cAMP Alters Odor Coding Across MB Neurons Heterogeneously. The MB lobes each contain hundreds of bundled axons (46, 48). Ca^{2+} responses at the lobe level therefore represent the net activation of numerous neurons by the odorant. To understand how individual neurons respond to elevation of cAMP, we imaged individual MB somata in the cell body layer (Fig. 4 *A* and *B*). A panel of Gal4 and split-Gal4 drivers was used to target GCaMP6f to particular subsets of MB neurons, and odor-evoked

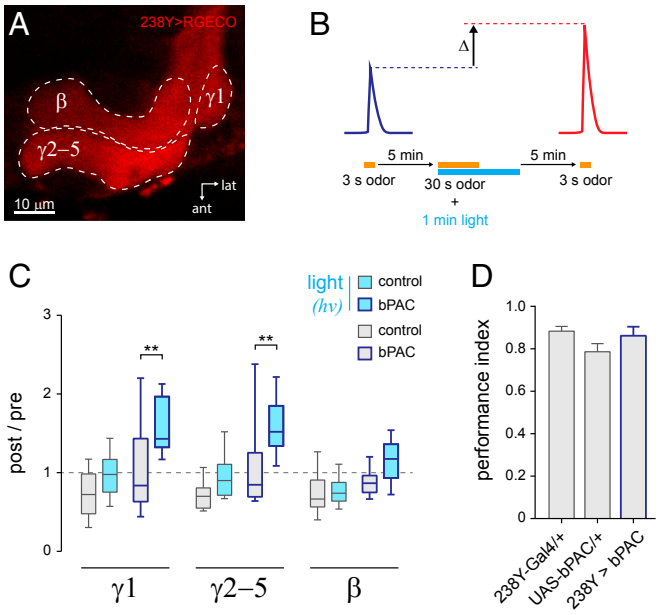

Fig. 3. Optogenetic stimulation of cAMP production in MB neurons generated plasticity in odor-evoked Ca^{2+} responses in MB γ-neurons. (*A*) Red-shifted Ca^{2+} reporter R-GECO expression in the MB γ- and β-lobes. The heel (γ1) region was imaged in a separate region of interest from the γ2–5-subdivisions. (*B*) Ca^{2+} imaging and blue light stimulation protocol. Odor-evoked responses were imaged with R-GECO, and compared before and after pairing odor with blue light to activate bPAC. Both UAS-R-GECO and UAS-bPAC were coexpressed in the same MB neurons with the 238Y-Gal4 driver. Ethyl butyrate was presented as the odorant. (*C*) Box plots showing the change in odor-evoked Ca^{2+} responses following cAMP elevation with bPAC. Data from the control genotype lacking bPAC (w; UAS-R-GECO/+; 238Y/+) are shown in gray-outlined boxes (n = 19 to 22 per group). Data from the experimental genotype (w; UAS-bPAC/UAS-R-GECO; 238Y/+) are shown in dark blue-outlined boxes (n = 20 per group). Blue light was used to activate bPAC (when present), and is indicated by the cyan box fill. $^{**}P < 0.01$ (Sidak). (*D*) Behavioral olfactory aversive classical conditioning in flies expressing bPAC in the MB (without light stimulation). The experimental genotype (w; UAS-bPAC/+; 238Y-Gal4/+) was compared with both heterozygous control genotypes (238Y-Gal4/+ and UAS-bPAC/+). Groups of ∼50 flies were trained and tested behaviorally in a T maze (n = 7 or 8 per genotype).

Ca^{2+} responses were imaged pre- and postforskolin treatment. Among γ-neurons, odor-evoked responses decreased in saline controls and increased, on average, in forskolin-treated animals (Fig. 4 *D–F*). This pattern was consistent across three γ-selective Gal4 drivers (Fig. 4*F*). Pre vs. post responses were analyzed across neurons with linear regression (Fig. 4*G*). There was no significant difference in slopes of the regression lines between controls and forskolin-treated groups (P = 0.321), indicating that the magnitude of forskolin-induced facilitation did not depend on the preforskolin odor response. The elevation of the regression line was significantly higher in the forskolin group ($P < 0.001$), reflecting an overall increase in odor-evoked responses. However, there was clear heterogeneity in changes between individual neurons—while most neurons exhibited increases following forskolin treatment, some decreased (Fig. 4*G*). To further examine this, neurons were categorized according to their change in odor-evoked responses following treatment. Most neurons in saline controls exhibited no significant change across odor presentations (n = 108/195) (Fig. 4*H*). Among the minority of neurons that exhibited a significant change, more decreased (n = 65) than increased (n = 22). This underlies the modest decrease in averaged responses (Fig. 4*E*). When cAMP was elevated with forskolin, the most common response was a significant increase in posttreatment responses (n = 157/292), though nearly as many neurons exhibited no change (n = 122), and a few decreased (n = 13) (Fig. 4*H*). These data suggest that elevation of cAMP exerts heterogeneous effects across individual MB γ neurons, with the net effect of biasing olfactory responses upward.

Similar to γ-neurons, α/β-neurons exhibited slight decreases in overall odor responses in controls, and significant increases in responses following cAMP elevation (Fig. 4 *I–K*). Two of three α/β-selective Gal4 drivers exhibited a significant increase, while the third showed a trend in the same direction (Fig. 4*K*). Linear regression revealed a significant increase in intercept ($P < 0.001$) but no change in slope (P = 0.329) (Fig. 4*L*). When categorized in terms of pre vs. post responses, in saline control experiments most α/β-neurons exhibited no change (n = 105/208) or decreases (n = 78), with a small number showing increases (n = 25). In forskolin-treated animals, most neurons increased (n = 110/260), a similar number exhibited no change (n = 107), and a few decreased (n = 43). Thus, as with the γ-neurons, α/β-neurons showed heterogeneous responses following cAMP manipulation that are biased toward facilitation. We additionally examined the third major class of MB neurons, α′/β′. (Fig. S4). This class of neuron exhibited no net change in odor-evoked responses following forskolin application, imaged using either cytosolic or presynaptically tethered GCaMP variants (Fig. S4 *B–D*). However, examination of single-cell responses revealed significant spontaneous activity, particularly following forskolin application (Fig. S4 *E* and *F*), as well as little correlation between calculated pre- and postforskolin response magnitudes (r^2 = 0.06) (Fig. S4*I*). This observation is broadly consistent with prior observations that α′/β′-neurons are more excitable than the other classes of MB neurons (42).

To comprehensively delineate the plasticity in intrinsic MB neurons following cAMP manipulation, we implemented activity-dependent neuronal labeling with CaMPARI (Fig. S5). This allowed us to produce a three-dimensional "activity snapshot" of MB neuron activity following cAMP elevation. MB γ- and α/β-neurons were targeted separately, driving UAS-CaMPARI (61) with subset-selective Gal4 drivers (1471 and c739, respectively). Significant increases in the number of labeled neurons were observed in forskolin-treated animals among both γ- and α/β-neurons (Fig. S5*D*). Since any given odor activates 6 ± 5% of MB neurons (42, 62), ∼37 γ-neurons (1471) and ∼60 α/β-neurons (c739) should respond to a typical odorant (48). Our data are consistent with this prediction, with a mean of 37.4 γ- and 77.6 α/β-neurons activated per MB in saline controls. Following forskolin treatment, CaMPARI labeled more neurons: Means of 83.2 γ-neurons and 111.7 α/β-neurons were labeled (Fig. S4*D*). This could reflect additional neurons "recruited" into the odor representation, though we saw no widespread changes in the number of responsive neurons in single-cell GCaMP imaging experiments. Therefore, the difference in the number of labeled cells is likely driven by differences in the number of neurons exhibiting odor-evoked activity levels that exceed the CaMPARI threshold. There was a larger percentage increase in the number of labeled cells following forskolin treatment among γ-neurons (122% increase) than α/β-neurons (44% increase), consistent with the interpretation that γ-neurons are more sensitive to elevation of cAMP. Overall, these data support the conclusion that cAMP increases the net responsivity of MB neurons to odorants, with differential effects across anatomical classes of MB neurons.

Aversive Conditioning Produces No Net Plasticity in the Mushroom Body. A major question is how cAMP-dependent plasticity functions during learning to encode memory. To answer this question, we first tested how aversive classical conditioning alters odor-evoked responses in the MB. Odor responses were imaged with GCaMP6f before and after pairing the odor with electric shocks delivered to the legs/abdomen (Fig. 5 *A* and *B*). Responses to the paired odor (CS+) or unpaired odor (CS−) were imaged in separate experiments (Fig. 5*B*). This paradigm allowed

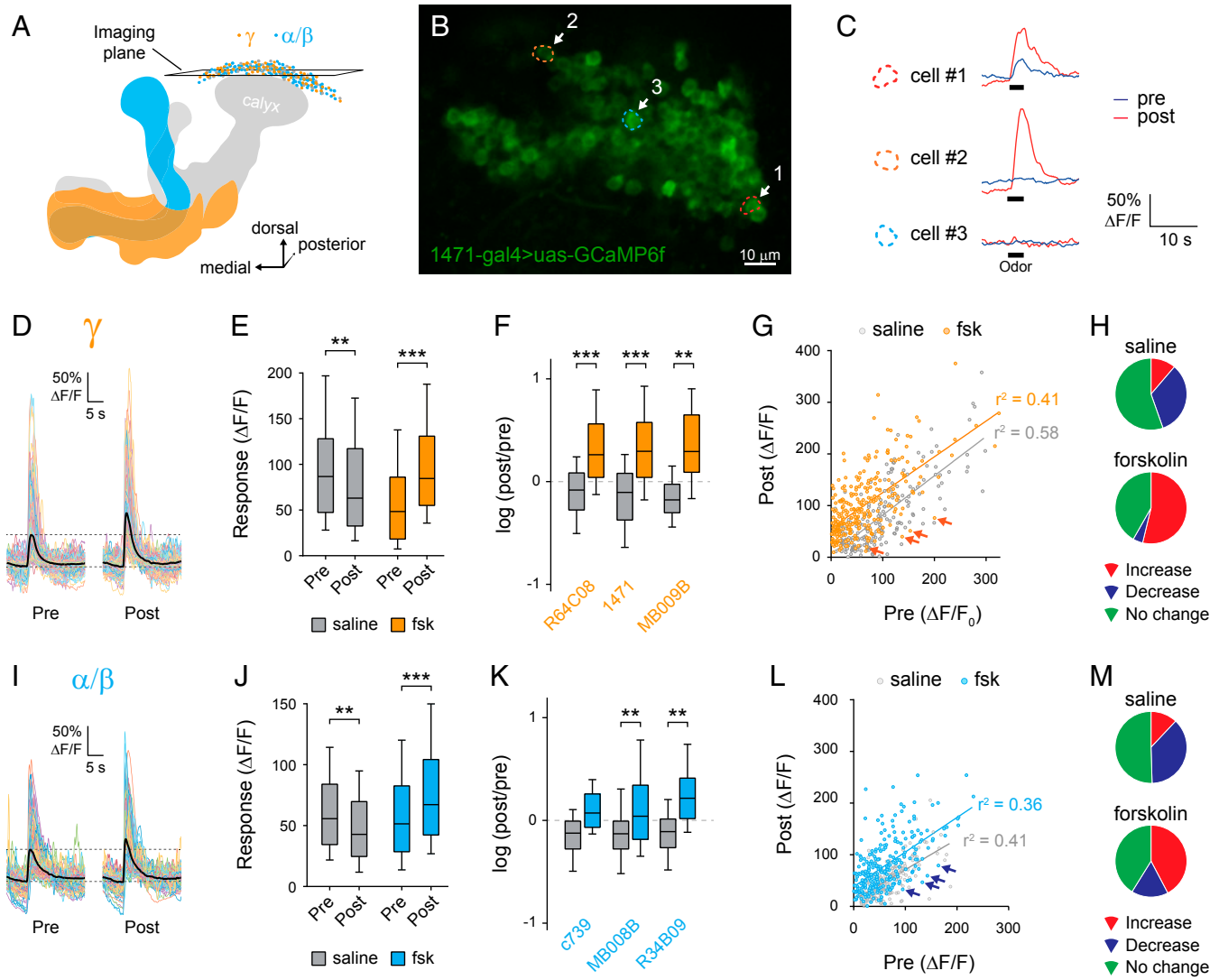

Fig. 4. Cyclic-AMP elevation altered odor coding heterogeneously across single MB γ- and α/β-neurons. (*A*) Drawing of a frontal view of the MB, with the lobes and somata of α/β- and γ-neurons indicated with cyan and orange, respectively. (*B*) Horizontal confocal section of MB somata, expressing GCaMP6f under control of the γ-selective 1471-Gal4 driver. (*C*) Odor-evoked Ca^{2+} responses, before (pre) and after (post) cAMP elevation with forskolin, from the three neurons outlined in *B*. Ethyl butyrate was presented as the odorant. (*D*) Time series traces showing the responses of individual MB γ-neurons pre and post cAMP elevation. GCaMP was expressed under the γ-selective drivers 1471, R64C08, or MB009B, and traces from all three drivers are pooled here. (*E*) Magnitude of single-neuron, odor-evoked Ca^{2+} responses, pre and post forskolin application in MB γ-neurons (forskolin $n = 292$; saline $n = 195$). $^{**}P < 0.01$, $^{***}P < 0.001$ (Sidak). (*F*) Change in odor-evoked Ca^{2+} responses among individual γ-neurons using three drivers: R64C08 (saline $n = 75$ neurons; forskolin $n = 126$), 1471 (saline $n = 67$; forskolin $n = 95$), or MB009B (saline $n = 53$; forskolin $n = 71$). $^{**}P < 0.01$, $^{***}P < 0.001$ (Sidak). (*G*) Posttreatment Ca^{2+} response magnitude graphed against the pretreatment response in γ-neurons, comparing forskolin and saline groups. Arrows highlight selected neurons that exhibited decreases in odor-evoked responses, and linear regression lines are plotted. (*H*) Single-cell responses of γ-neurons, categorized by change in response following treatment (no change, increase, or decrease). (*I*) Time series traces showing the responses of individual MB α/β-neurons pre and post cAMP elevation. (*J*) Magnitude of single-neuron, odor-evoked Ca^{2+} responses, pre and post forskolin application in MB α/β-neurons. $^{**}P < 0.01$, $^{***}P < 0.001$ (Sidak). (*K*) Change in odor-evoked Ca^{2+} responses among α/β-neurons using three drivers: c739 (saline $n = 71$ neurons; forskolin $n = 84$), R34B09 (saline $n = 57$; forskolin $n = 91$), and MB008B (saline $n = 80$; forskolin $n = 85$). $^{**}P < 0.01$ (Sidak). (*L*) Posttreatment Ca^{2+} response magnitude graphed against the pretreatment response in α/β-neurons, plotted as in *G*. (*M*) Single-cell responses of α/β-neurons, plotted as in *H*.

within-animal comparison of the odor-evoked responses before and after conditioning, as well as comparison of the group differences in CS+ vs. CS− responses. Across the MB, responses to both the CS+ and CS− were reduced following conditioning, representing nonassociative adaptation (Fig. 5 *C* and *D*). The Ca^{2+} responses did not significantly differ between the CS+ and CS− across any region imaged, suggesting that aversive conditioning does not produce a net change in MB neurons across the lobes (Fig. 5*E*). Further subdivision of the γ- and β-lobes did not reveal compartment-specific effects (Fig. 5*G*). There was a trend toward less adaptation in CS− responses, particularly among the α- and β-lobes. Therefore, we tested conditioning effects in *rut*^{1} mutants, which have a mutation in the type I adenylyl cyclase and exhibit impaired olfactory learning and memory (63–65). In these mutants, no significant differences were observed across any of the regions imaged (Fig. 5*F*), though there was a trend in the opposite direction relative to the wild-type flies (less adaptation in the CS+ responses). In an additional test, we starved flies before aversive conditioning, which can stabilize memory following single-cycle aversive training (66). Similar to the other protocols tested, this paradigm produced no differences in CS+ vs. CS− responses (Fig. 5*H*). In summary, we were unable to detect significant changes in

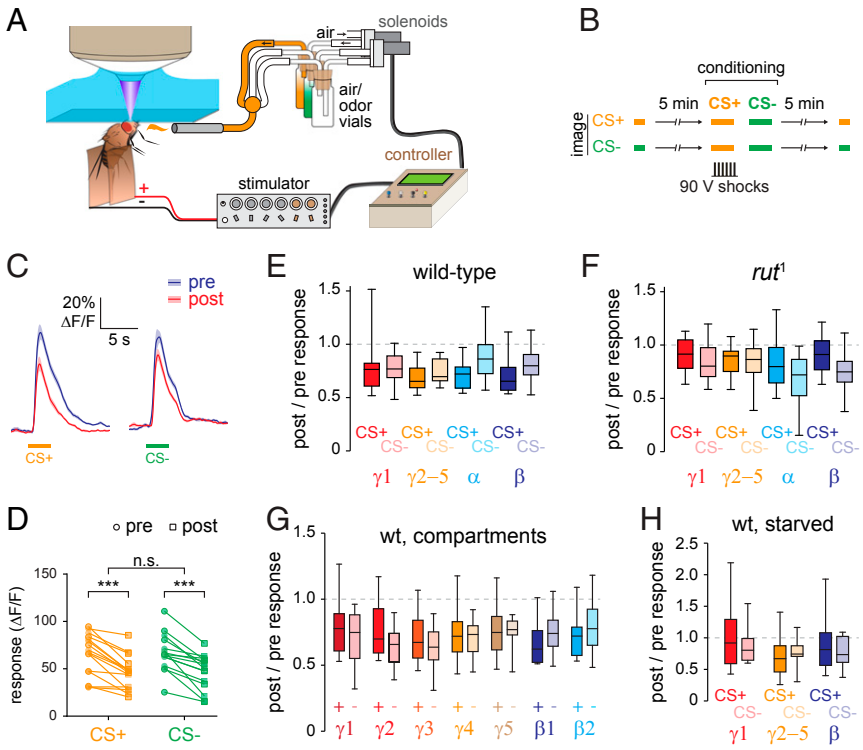

Fig. 5. Aversive conditioning does not produce detectable changes in odor coding across the MB. (*A*) Drawing of the in vivo aversive conditioning apparatus. (*B*) Schematic of the experimental protocol. (*C*) Comparison of pre- and postconditioning responses to the CS+ and CS− in the γ-lobe (mean ± SEM). (*D*) Pre- and postconditioning responses to the CS+ (ethyl butyrate) and CS− (isoamyl acetate) in the γ-lobe of each animal. ***$P < 0.001$ (Sidak); n.s., not significant. (*E*) Comparison of changes in odor responses following conditioning in wild-type flies ($n \geq 16$), plotted as the ratio of post:pre responses. (*F*) Comparison of changes in odor responses following conditioning in *rut*^{1} mutant flies ($n = 12$). (*G*) Subregion analysis of aversive conditioning effects in the MB γ- and β-lobes of wild-type flies. Data are from the same flies as in *E*. (*H*) Comparison of changes in odor responses following conditioning in wild-type flies ($n = 12$), starved for 18 to 24 h before testing.

net odor-evoked Ca^{2+} responses associated with aversive conditioning. While we observed no effect at the cellular level, this remains broadly consistent with models emphasizing localized synaptic plasticity at MB output synapses during aversive conditioning, which may be regulated in a highly localized, synapse-specific manner (11, 35, 67).

Appetitive Conditioning Drives Robust, Rutabaga-Dependent Plasticity. Prior studies have demonstrated a critical role for cAMP signaling in intrinsic MB neurons in learning, yet we were unable to detect net plasticity during aversive conditioning. Conceptually, the MB is critical for olfactory associative memory and integration of conditioned/unconditioned stimulus cues, but has also been implicated in more general motivational control and context dependence of behavior (68–71). In addition, there are differences in functional circuit requirements for appetitive vs. aversive conditioning (4, 5, 7, 8, 28, 49, 72, 73). Therefore, we reasoned that appetitive conditioning may exert broad influence over MB neuron responsivity. To test this, we paired odor with sucrose reward in hungry flies (Fig. 6 *A* and *B*). Following conditioning, the post:pre ratio was significantly enhanced, for the CS+ relative to the CS−, across all regions imaged (γ1, γ2 to γ5, α, and β) (Fig. 6 *C* and *D*). Responses to the CS− dropped after conditioning, reflecting a similar adaptation as seen with both odors during aversive conditioning. However, the CS+ response was enhanced relative to the baseline adaptation (Fig. 6*H*). This was consistent regardless of which odor was used as the CS+ and CS− (Fig. 6 *D* and *F*), and was absent when odor was presented without reinforcement (Fig. 6*G*). These data suggest that appetitive conditioning produces an associative change in the magnitude of the responses to the CS+ and CS−, increasing relative responses of the MB to the trained odor (↑ CS+:CS−). To determine whether the plasticity was dependent on cAMP signaling via the Rutabaga adenylyl cyclase, we tested *rut*^{1} mutants, which are impaired in appetitive (in addition to aversive) learning (7, 65, 73, 74). In *rut*^{1} mutants, the difference between the CS+ and CS− responses was abolished across all of the regions examined (Fig. 6 *E* and *I*). To test whether there was any regional variation across the subdomains of these lobes, we further parsed the β- and γ-lobes into individual compartments (Fig. 6*J*). CS+ responses were significantly elevated relative to CS− responses in the proximal γ-compartments (γ1, γ2) and distal β-compartment (β2) (Fig. 6*K*). Differences between CS+ and CS− in other compartments did not reach significance, though in all cases there was a trend in the same direction.

We next asked what effect appetitive conditioning produces on cAMP, and sought to mimic the naturalistic cAMP levels with pharmacological cAMP manipulations. To measure cAMP levels during learning, we utilized the genetically encoded, fluorescence resonance energy transfer (FRET)-based cAMP reporter UAS-epac-cAMPs, expressed in the MB under control of the 238Y-Gal4 driver (75, 76). cAMP levels were measured in the γ2–5-region while presenting odor and sucrose, which were paired for 30 s (Fig. 7*A*). This appetitive conditioning protocol produced a robust response in the cAMP reporter (12.7 ± 6.4% $\Delta R/R$) (Fig. 7*A*). We then imaged cAMP while applying forskolin in the bath (Fig. 7 *A* and *B*). Several concentrations were tested, increasing in quarter-log-unit intervals. Since the kinetics of the cAMP responses differed between the naturalistic training and the pharmacological manipulation, we compared peak amplitudes of the cAMP responses. Among the concentrations tested, 30 μM forskolin (13.3 ± 2.0% $\Delta R/R$) most closely approximated the peak cAMP responses evoked by appetitive conditioning,

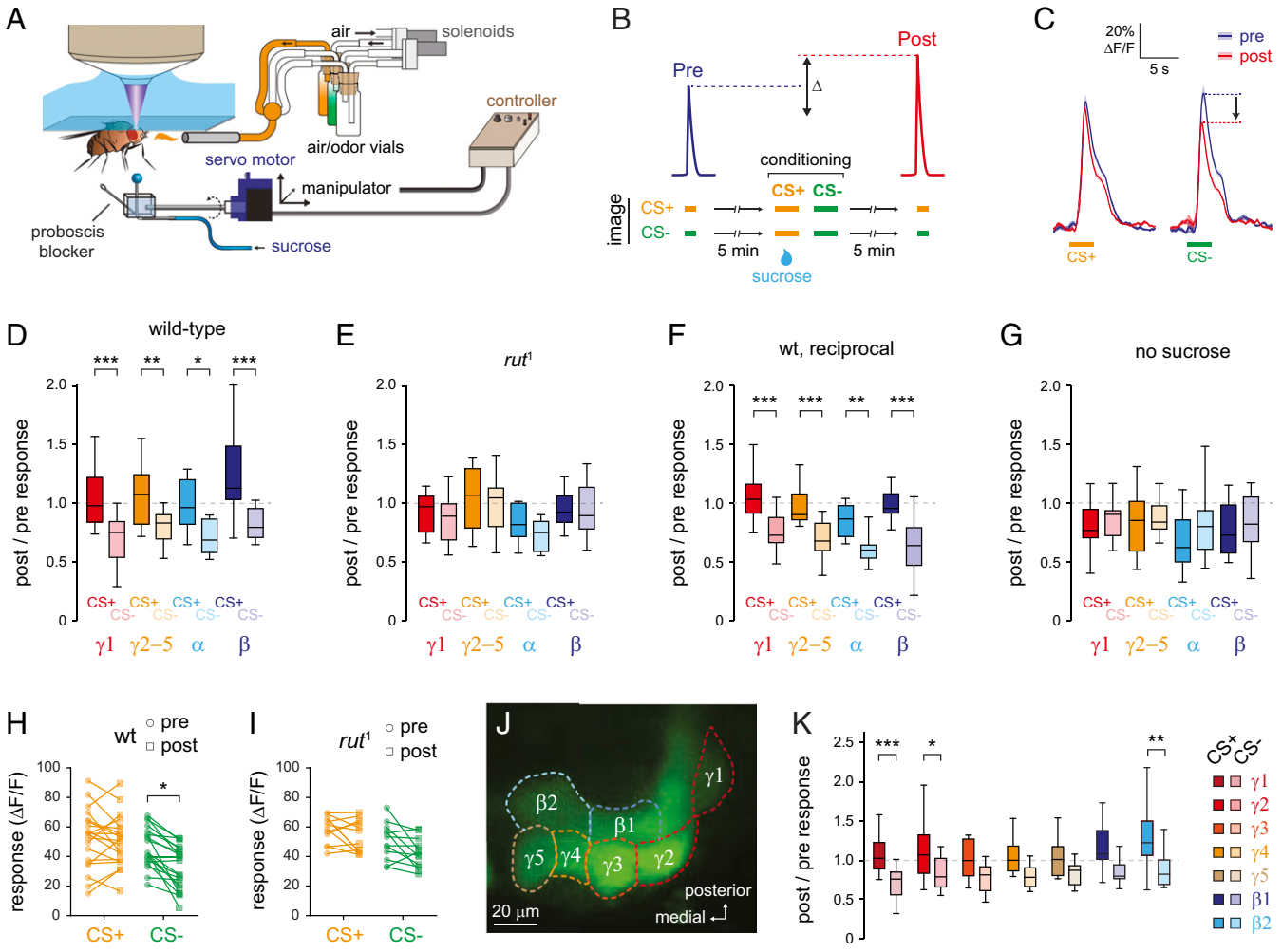

Fig. 6. Appetitive conditioning drives a change in MB responses, altering the balance of odor responses to the CS+ and CS−. (*A*) Drawing of the in vivo appetitive conditioning apparatus. (*B*) Schematic of the appetitive conditioning experimental protocol. (*C*) Comparison of pre- and postconditioning responses to the CS+ (ethyl butyrate; EB) and CS− (isoamyl acetate; IAA) in the γ-lobe of wild-type flies (EB*, IAA) (mean ± SEM). (*D*) Appetitive conditioning in wild-type flies. Comparison of changes in odor responses following appetitive conditioning (EB*, IAA) ($n \geq 13$). *$P < 0.05$, **$P < 0.01$, ***$P < 0.001$ (Sidak). (*E*) Appetitive conditioning in *rutabaga* mutants ($n = 12$ per group), as in *D*. (*F*) Appetitive conditioning in wild-type (wt) flies with reciprocal conditioning (IAA*, EB) ($n \geq 13$). **$P < 0.01$, ***$P < 0.001$ (Sidak). (*G*) Comparison of changes in odor responses following odor presentation without sucrose reinforcement ($n \geq 12$). (*H*) Pre- and postconditioning responses to the CS+ and CS− in the γ1-region of wild-type flies. *$P < 0.05$ (Sidak). (*I*) Pre- and postconditioning responses to the CS+ and CS− in the γ-lobe of each *rut*^{1} animal. (*J*) Confocal image of the γ- and β-lobes, with ROIs around each subdomain. (*K*) Subdomain analysis of appetitive conditioning effects in the MB γ- and β-lobes of wild-type flies. *$P < 0.05$, **$P < 0.01$, $P < 0.001$ (Sidak).

and the magnitudes of the two did not significantly differ ($P > 0.05$; Sidak). Therefore, we used that forskolin concentration to test whether elevating cAMP to behaviorally relevant levels affected odor responsivity in the MB. Odor-evoked Ca^{2+} responses in the MB γ-lobe were significantly facilitated following pairing of odor with elevation of cAMP using 30 μM forskolin (Fig. 7*C*). This change was compared with flies exposed to the control drug 1,9-dideoxyforskolin, a forskolin analog that does not elevate cAMP. The post:pre ratio was significantly larger in flies exposed to 30 μM forskolin than in controls exposed to 30 μM 1,9-dideoxyforskolin, in agreement with previous results (8). Overall, these data suggest that appetitive conditioning elevates cAMP in MB neurons, and that mimicking this level of cAMP elevation produces plasticity in the MB.

Discussion

The present data support several major conclusions about the role of cAMP-dependent plasticity in the memory-encoding MB: (*i*) Intrinsic MB neurons exhibit robust cAMP-dependent plasticity; (*ii*) cAMP-dependent plasticity is heterogeneous, both across and within anatomical classes of MB neurons; (*iii*) the directionality and magnitude of plasticity parallel Rut-dependent associative changes in MB responsivity following appetitive classical conditioning; and (*iv*) appetitive conditioning produces changes in cAMP of a magnitude that generates plasticity in odor-evoked responses. Thus, cAMP-dependent plasticity plays a major role in modulating intrinsic MB neurons, directly linking the physiology of MB neurons to the behavioral roles for cAMP signaling molecules in learning and memory (8, 9, 12, 17, 23, 24, 77–79). One caveat to the interpretation of imaging studies is that the preparations require tethering the animal under a microscope. Future developments enabling recording of brain activity in freely behaving animals will be necessary to test how responses in the MB neurons facilitate behavioral output in real time.

In the context of olfactory learning, the MB encodes a sparse representation of olfactory space, which is computationally advantageous for learning and potentially modulated by learned valence (11, 40, 42–44, 49, 80). If neurons responded homogeneously

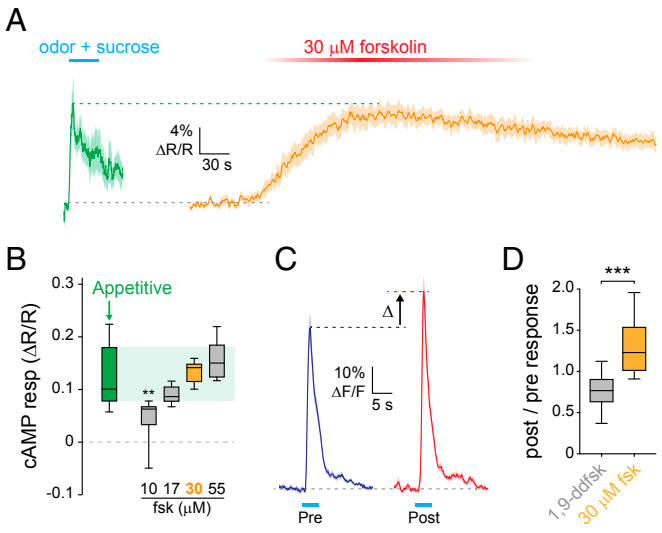

Fig. 7. Quantitative comparison of appetitive conditioning and cAMP-dependent plasticity in vivo. (*A*) Comparison of cAMP responses evoked by appetitive conditioning and 30 μM forskolin application. The inverse FRET ratio (CFP/YFP) ($\Delta R/R$) is plotted (mean ± SEM). Appetitive conditioning-induced cAMP responses (n = 7) (*Left*) and fsk responses (*Right*) (n = 6). (*B*) Quantification of peak cAMP responses during appetitive conditioning, and with fsk across quarter-log-unit intervals (n = 7 each). $^{**}P < 0.01$ relative to appetitive conditioning (Sidak). (*C*) Odor-evoked Ca^{2+} responses in the MB γ-lobe before and after elevation of cAMP with 30 μM forskolin (n = 20). Odor presentation time is indicated with the cyan bar. The post response was significantly elevated ($P < 0.05$; Mann–Whitney). (*D*) Comparison of the change in odor-evoked responses in the MB γ-lobe in flies following application/washout of forskolin or 1,9-dideoxyforskolin (1,9-ddfsk), both at 30 μM (n = 20). $^{***}P < 0.001$ (Mann–Whitney).

to input stimuli, coincidence detection would result in uniform plasticity across the sparse set of neurons that encode the odor and receive a reinforcement signal (9, 24, 38). However, the heterogeneity we observed in cAMP-dependent plasticity suggests that olfactory memory traces may be driven to specific subsets of "eligible" neurons in the MB. This could play an analogous role to memory allocation, which drives memory traces to subsets of eligible neurons in the mammalian amygdala during fear conditioning (81, 82). Molecularly, heterogeneity may be driven by differential expression of genes that function downstream of cAMP/Epac/PKA to regulate neuronal excitability or presynaptic function. Such differences in expression could be set up via developmental or epigenetic mechanisms.

We propose that the cAMP-dependent plasticity in the MB plays two roles during olfactory learning: filtering MB responses based on salience and encoding valence (Fig. S6). A role for MB plasticity in salience filtering is suggested by the observation that appetitive conditioning produced enhancement of MB responses across spatial compartments. These compartments have been suggested to route olfactory signals to valence-encoding output neurons, driving learned approach or avoidance (49) via heterosynaptic plasticity (11). Therefore, the broad pattern of plasticity observed here would affect multiple downstream output pathways of opposing valence, suggesting that it does not encode valence per se. Rather, it may function to heighten relative MB sensitivity to salient stimuli. Across multiple sensory systems, ascending information is filtered according to salience, typically enhancing responses to stimuli that are biologically important (83). Alternatively, appetitive conditioning may modulate MB neurons in a fundamentally different way from aversive conditioning. While these opposing forms of memory require many overlapping MB-associated neurons, there are some differences in the circuits recruited during these forms of learning (4, 5, 7, 8, 28, 49, 72, 73), and plasticity across MB neurons may be one difference. Regardless of the interpretation, our data reveal cAMP-dependent plasticity at the cellular level in intrinsic MB neurons. This may be layered on top of synaptic plasticity at MB output synapses, which have been proposed to encode valence by altering how olfactory signals flow through the neuronal networks that mediate behavioral approach or avoidance (11, 38, 44) (Fig. S6).

Several additional lines of evidence support the idea that cAMP-dependent plasticity serves as an overall gain control, regulating MB responses based on stimulus salience. First, the MB and MB-innervating dopaminergic neurons modulate salience-based decision making in a visual flight simulator paradigm (84). Second, dopaminergic neurons innervating the MB respond broadly to sensory stimuli that do not have an acquired valence (85, 86), and exhibit activity that is correlated with locomotion (67, 87). Activation of these neurons elevates cAMP in the downstream MB neurons in a compartmentalized manner (8), which in turn modulates their sensitivity and neurotransmission at the MB–MBON synapses (8, 11, 24, 40, 67). Thus, the MB neurons receive dynamically regulated dopaminergic inputs that alter the function of both the MB and downstream network components as a function of behavioral state. This may facilitate learning in situations in which the animal is likely to experience biologically important events (e.g., during foraging). Similar modulatory mechanisms modulate plasticity and memory in other animals as well. For instance, in honeybees, appetitive conditioning prolongs odor responses in MB neurons (88). Likewise, in the mammalian amygdala, coactivation of neuromodulatory and Hebbian plasticity is necessary for plasticity and memory (89).

Aversive conditioning produced no significant plasticity in our hands, consistent with results from some optogenetic reinforcement substitution imaging experiments (11). However, since Rut is required in MB neurons for normal aversive memory (12, 16), cAMP-dependent plasticity is likely present in some form. Indeed, a previous study detected plasticity in the γ-lobe following aversive conditioning (35), which could be tightly localized to specific output synapses or neuronal subsets (11, 49, 67). Pairing odor with stimulation of tyrosine hydroxylase Gal4-labeled dopaminergic neurons produces aversive memory and detectable plasticity in MB γ-neurons (2, 3, 5, 8). In this study, we observed robust plasticity differentially following appetitive conditioning. This may be due to a bias toward learning about stimuli that guide motivationally relevant behaviors, such as approaching food-associated odors. Consistent with such an interpretation, appetitive conditioning produces memory that is more stable over time than aversive memory (65, 90). A single trial of appetitive conditioning leads to the formation of long-term memory, while aversive conditioning requires multiple-spaced trials. The cAMP-dependent plasticity during appetitive conditioning could trigger downstream molecular pathways necessary to engage long-term memory formation. This presumably interacts with Ca^{2+} levels in neurons to regulate short- and long-term memory. In honeybees, elevating intracellular Ca^{2+} during a single-trial conditioning, which normally only triggers short-term memory, can induce long-term memory, whereas decreasing intracellular Ca^{2+} during multiple-spaced training impaired long-term memory formation (91). In addition, appetitive memory retrieval is motivationally gated by hunger state, suggesting a tie-in with motivational state (71). Integrating our observations, this suggests that motivationally relevant stimuli may enhance the sensitivity of MB neurons via cAMP-dependent plasticity, modulating the overall gain of the system in a salience-dependent manner.

The MB is involved in multiple distinct yet potentially interrelated behaviors, including several forms of learning and memory (20, 71, 79, 92–94), regulating sleep and activity (49, 95–97), context generalization (70), habituation (98), temperature

preference (86, 99), context dependence of olfactory behaviors (68, 69), and salience-based decision making (84). The common thread among these behaviors is that they revolve around selection of an appropriate action based on context. Thus, a primary function of the MB and its modulatory input may to be alter the probability of action based on integrating environmental cues and internal state. In such a scenario, modulating the overall gain of the circuit could function in concert with fine-scale synapse-specific plasticity to alter the flow of information to downstream motor areas. Thus, our data support a model in which dopaminergic neurons and downstream cAMP-dependent plasticity modulate MB responses to stimuli based on their salience, priming the animal to engage in appropriate goal-oriented behaviors.

Materials and Methods

Detailed procedures can be found in *SI Materials and Methods*. Briefly, flies were raised according to standard laboratory protocols. For in vivo imaging, flies were mounted in an imaging chamber, a cuticle window was opened, and the brain was imaged with appropriate laser lines under a confocal microscope. Saline was perfused across the brain throughout, and pharmacological manipulations were applied in the saline. Genetically encoded Ca^{2+}/cAMP reporters or optogenetic effectors were expressed in MB neurons or olfactory projection neurons under Gal4 control. Responses were plotted as the baseline-normalized change in GCaMP fluorescence ($\Delta F/F$) or inverse FRET ratio ($\Delta R/R$). Forskolin was used to elevate cAMP, and pre/post odor-evoked responses were imaged as previously described (8). For optogenetic elevation of cAMP, R-GECO (60) and bPAC (59) were coexpressed in MB neurons, and the brain was illuminated with blue laser light (448 nm). For activity-dependent neuronal tagging in vivo, CaMPARI was expressed in the MB. Odor was presented and then paired with forskolin or saline, a *z* stack encompassing the complete region of the MB somata was collected, and the number of photoconverted cells was counted. To combine in vivo imaging and aversive conditioning, flies were prepared for in vivo imaging and trained with a modified aversive classical conditioning paradigm under the microscope (30–32). Similarly, imaging was combined with appetitive conditioning by pairing odor with sucrose reward under the microscope in a differential conditioning paradigm; MB responses were imaged with GCaMP or epac-cAMPs. Statistical analysis was performed with GraphPad Prism.

ACKNOWLEDGMENTS. We thank Ronald L. Davis, Andre Fiala, Martin Schwaerzel, and the Bloomington *Drosophila* Stock Center (NIH P400D018537) for fly stocks. Martin Schwaerzel provided helpful feedback on photoactivatable adenylyl cyclases. Gal4 drivers and split-Gal4 drivers from the Janelia collection were kindly provided by Yoshinori Aso and Gerald Rubin; relevant enhancer fragments and expression patterns are as previously described (50, 100) (https://www.janelia.org/project-team/flylight). Research support was provided by the NIH (NIH/NIMH R00MH092294) and Whitehall Foundation, and T.L. and T.B. are Neuroscience Scholars of the Esther B. O'Keeffe Charitable Foundation.

1. Rosenkranz JA, Grace AA (2002) Dopamine-mediated modulation of odour-evoked amygdala potentials during pavlovian conditioning. *Nature* 417:282–287.
2. Schroll C, et al. (2006) Light-induced activation of distinct modulatory neurons triggers appetitive or aversive learning in *Drosophila* larvae. *Curr Biol* 16:1741–1747.
3. Aso Y, et al. (2010) Specific dopaminergic neurons for the formation of labile aversive memory. *Curr Biol* 20:1445–1451.
4. Liu C, et al. (2012) A subset of dopamine neurons signals reward for odour memory in *Drosophila*. *Nature* 488:512–516.
5. Claridge-Chang A, et al. (2009) Writing memories with light-addressable reinforcement circuitry. *Cell* 139:405–415.
6. Ichinose T, et al. (2015) Reward signal in a recurrent circuit drives appetitive long-term memory formation. *Elife* 4:e10719.
7. Schwaerzel M, et al. (2003) Dopamine and octopamine differentiate between aversive and appetitive olfactory memories in *Drosophila*. *J Neurosci* 23:10495–10502.
8. Boto T, Louis T, Jindachomthong K, Jalink K, Tomchik SM (2014) Dopaminergic modulation of cAMP drives nonlinear plasticity across the *Drosophila* mushroom body lobes. *Curr Biol* 24:822–831.
9. Gervasi N, Tchénio P, Preat T (2010) PKA dynamics in a *Drosophila* learning center: Coincidence detection by rutabaga adenylyl cyclase and spatial regulation by dunce phosphodiesterase. *Neuron* 65:516–529.
10. Kim YC, Lee HG, Han KA (2007) D1 dopamine receptor dDA1 is required in the mushroom body neurons for aversive and appetitive learning in *Drosophila*. *J Neurosci* 27:7640–7647.
11. Hige T, Aso Y, Modi MN, Rubin GM, Turner GC (2015) Heterosynaptic plasticity underlies aversive olfactory learning in *Drosophila*. *Neuron* 88:985–998.
12. Zars T, Fischer M, Schulz R, Heisenberg M (2000) Localization of a short-term memory in *Drosophila*. *Science* 288:672–675.
13. McGuire SE, Le PT, Osborn AJ, Matsumoto K, Davis RL (2003) Spatiotemporal rescue of memory dysfunction in *Drosophila*. *Science* 302:1765–1768.
14. Qin H, et al. (2012) Gamma neurons mediate dopaminergic input during aversive olfactory memory formation in *Drosophila*. *Curr Biol* 22:608–614.
15. Trannoy S, Redt-Clouet C, Dura JM, Preat T (2011) Parallel processing of appetitive short- and long-term memories in *Drosophila*. *Curr Biol* 21:1647–1653.
16. Mao Z, Roman G, Zong L, Davis RL (2004) Pharmacogenetic rescue in time and space of the rutabaga memory impairment by using Gene-Switch. *Proc Natl Acad Sci USA* 101:198–203.
17. Blum AL, Li W, Cressy M, Dubnau J (2009) Short- and long-term memory in *Drosophila* require cAMP signaling in distinct neuron types. *Curr Biol* 19:1341–1350.
18. Akalal DB, et al. (2006) Roles for *Drosophila* mushroom body neurons in olfactory learning and memory. *Learn Mem* 13:659–668.
19. Pavot P, Carbognin E, Martin JR (2015) PKA and cAMP/CNG channels independently regulate the cholinergic Ca(2+)-response of *Drosophila* mushroom body neurons. *eNeuro* 2:ENEURO.0054-14.2015.
20. Niewalda T, et al. (2015) Synapsin determines memory strength after punishment- and relief-learning. *J Neurosci* 35:7487–7502.
21. Richlitzki A, Latour P, Schwärzel M (2017) Null EPAC mutants reveal a sequential order of versatile cAMP effects during *Drosophila* aversive odor learning. *Learn Mem* 24:210–215.
22. Michels B, et al. (2011) Cellular site and molecular mode of synapsin action in associative learning. *Learn Mem* 18:332–344.
23. Skoulakis EM, Kalderon D, Davis RL (1993) Preferential expression in mushroom bodies of the catalytic subunit of protein kinase A and its role in learning and memory. *Neuron* 11:197–208.
24. Tomchik SM, Davis RL (2009) Dynamics of learning-related cAMP signaling and stimulus integration in the *Drosophila* olfactory pathway. *Neuron* 64:510–521.
25. Tomchik SM, Davis RL (2013) Memory research through four eras: Genetic, molecular biology, neuroanatomy, and systems neuroscience. *Invertebrate Learning and Memory*, eds Menzel R, Benjamin P (Elsevier, London), pp 359–377.
26. Akalal DB, Yu D, Davis RL (2010) A late-phase, long-term memory trace forms in the γ neurons of *Drosophila* mushroom bodies after olfactory classical conditioning. *J Neurosci* 30:16699–16708.
27. Akalal DB, Yu D, Davis RL (2011) The long-term memory trace formed in the *Drosophila* α/β mushroom body neurons is abolished in long-term memory mutants. *J Neurosci* 31:5643–5647.
28. Cervantes-Sandoval I, Davis RL (2012) Distinct traces for appetitive versus aversive olfactory memories in DPM neurons of *Drosophila*. *Curr Biol* 22:1247–1252.
29. Liu X, Davis RL (2009) The GABAergic anterior paired lateral neuron suppresses and is suppressed by olfactory learning. *Nat Neurosci* 12:53–59.
30. Yu D, Akalal DB, Davis RL (2006) *Drosophila* alpha/beta mushroom body neurons form a branch-specific, long-term cellular memory trace after spaced olfactory conditioning. *Neuron* 52:845–855.
31. Yu D, Keene AC, Srivatsan A, Waddell S, Davis RL (2005) *Drosophila* DPM neurons form a delayed and branch-specific memory trace after olfactory classical conditioning. *Cell* 123:945–957.
32. Yu D, Ponomarev A, Davis RL (2004) Altered representation of the spatial code for odors after olfactory classical conditioning: Memory trace formation by synaptic recruitment. *Neuron* 42:437–449.
33. Wang Y, Mamiya A, Chiang AS, Zhong Y (2008) Imaging of an early memory trace in the *Drosophila* mushroom body. *J Neurosci* 28:4368–4376.
34. Tan Y, Yu D, Pletting J, Davis RL (2010) Gilgamesh is required for rutabaga-independent olfactory learning in *Drosophila*. *Neuron* 67:810–820.
35. Zhang S, Roman G (2013) Presynaptic inhibition of gamma lobe neurons is required for olfactory learning in *Drosophila*. *Curr Biol* 23:2519–2527.
36. McGuire SE, Le PT, Davis RL (2001) The role of *Drosophila* mushroom body signaling in olfactory memory. *Science* 293:1330–1333.
37. Dubnau J, Grady L, Kitamoto T, Tully T (2001) Disruption of neurotransmission in *Drosophila* mushroom body blocks retrieval but not acquisition of memory. *Nature* 411:476–480.
38. Heisenberg M (2003) Mushroom body memoir: From maps to models. *Nat Rev Neurosci* 4:266–275.
39. Séjourné J, et al. (2011) Mushroom body efferent neurons responsible for aversive olfactory memory retrieval in *Drosophila*. *Nat Neurosci* 14:903–910.
40. Hige T, Aso Y, Rubin GM, Turner GC (2015) Plasticity-driven individualization of olfactory coding in mushroom body output neurons. *Nature* 526:258–262.
41. Owald D, et al. (2015) Activity of defined mushroom body output neurons underlies learned olfactory behavior in *Drosophila*. *Neuron* 86:417–427.
42. Turner GC, Bazhenov M, Laurent G (2008) Olfactory representations by *Drosophila* mushroom body neurons. *J Neurophysiol* 99:734–746.
43. Campbell RA, et al. (2013) Imaging a population code for odor identity in the *Drosophila* mushroom body. *J Neurosci* 33:10568–10581.
44. Aso Y, et al. (2014) Mushroom body output neurons encode valence and guide memory-based action selection in *Drosophila*. *Elife* 3:e04580.

45. Pai TP, et al. (2013) *Drosophila* ORB protein in two mushroom body output neurons is necessary for long-term memory formation. *Proc Natl Acad Sci USA* 110: 7898–7903.
46. Crittenden JR, Skoulakis EM, Han KA, Kalderon D, Davis RL (1998) Tripartite mushroom body architecture revealed by antigenic markers. *Learn Mem* 5:38–51.
47. Tanaka NK, Tanimoto H, Ito K (2008) Neuronal assemblies of the *Drosophila* mushroom body. *J Comp Neurol* 508:711–755.
48. Aso Y, et al. (2009) The mushroom body of adult *Drosophila* characterized by GAL4 drivers. *J Neurogenet* 23:156–172.
49. Aso Y, et al. (2014) The neuronal architecture of the mushroom body provides a logic for associative learning. *Elife* 3:e04577.
50. Jenett A, et al. (2012) A GAL4-driver line resource for *Drosophila* neurobiology. *Cell Rep* 2:991–1001.
51. Pech U, Revelo NH, Seitz KJ, Rizzoli SO, Fiala A (2015) Optical dissection of experience-dependent pre- and postsynaptic plasticity in the *Drosophila* brain. *Cell Rep* 10:2083–2095.
52. Tian L, et al. (2009) Imaging neural activity in worms, flies and mice with improved GCaMP calcium indicators. *Nat Methods* 6:875–881.
53. Walker AS, Burrone J, Meyer MP (2013) Functional imaging in the zebrafish retinotectal system using RGECO. *Front Neural Circuits* 7:34.
54. Christiansen F, et al. (2011) Presynapses in Kenyon cell dendrites in the mushroom body calyx of *Drosophila*. *J Neurosci* 31:9696–9707.
55. Rolls MM, et al. (2007) Polarity and intracellular compartmentalization of *Drosophila* neurons. *Neural Dev* 2:7.
56. Pauls D, Selcho M, Gendre N, Stocker RF, Thum AS (2010) *Drosophila* larvae establish appetitive olfactory memories via mushroom body neurons of embryonic origin. *J Neurosci* 30:10655–10666.
57. Chen CC, et al. (2012) Visualizing long-term memory formation in two neurons of the *Drosophila* brain. *Science* 335:678–685.
58. Waddell S, Armstrong JD, Kitamoto T, Kaiser K, Quinn WG (2000) The amnesiac gene product is expressed in two neurons in the *Drosophila* brain that are critical for memory. *Cell* 103:805–813.
59. Stierl M, et al. (2011) Light modulation of cellular cAMP by a small bacterial photoactivated adenylyl cyclase, bPAC, of the soil bacterium *Beggiatoa*. *J Biol Chem* 286: 1181–1188.
60. Zhao Y, et al. (2011) An expanded palette of genetically encoded Ca^{2+} indicators. *Science* 333:1888–1891.
61. Fosque BF, et al. (2015) Labeling of active neural circuits in vivo with designed calcium integrators. *Science* 347:755–760.
62. Wang Y, et al. (2004) Stereotyped odor-evoked activity in the mushroom body of *Drosophila* revealed by green fluorescent protein-based Ca^{2+} imaging. *J Neurosci* 24: 6507–6514.
63. Levin LR, et al. (1992) The *Drosophila* learning and memory gene rutabaga encodes a Ca^{2+}/calmodulin-responsive adenylyl cyclase. *Cell* 68:479–489.
64. Livingstone MS, Sziber PP, Quinn WG (1984) Loss of calcium/calmodulin responsiveness in adenylate cyclase of rutabaga, a *Drosophila* learning mutant. *Cell* 37: 205–215.
65. Tempel BL, Bonini N, Dawson DR, Quinn WG (1983) Reward learning in normal and mutant *Drosophila*. *Proc Natl Acad Sci USA* 80:1482–1486.
66. Hirano Y, et al. (2013) Fasting launches CRTC to facilitate long-term memory formation in *Drosophila*. *Science* 339:443–446.
67. Cohn R, Morantte I, Ruta V (2015) Coordinated and compartmentalized neuromodulation shapes sensory processing in *Drosophila*. *Cell* 163:1742–1755.
68. Bräcker LB, et al. (2013) Essential role of the mushroom body in context-dependent CO_2 avoidance in *Drosophila*. *Curr Biol* 23:1228–1234.
69. Lewis LP, et al. (2015) A higher brain circuit for immediate integration of conflicting sensory information in *Drosophila*. *Curr Biol* 25:2203–2214.
70. Liu L, Wolf R, Ernst R, Heisenberg M (1999) Context generalization in *Drosophila* visual learning requires the mushroom bodies. *Nature* 400:753–756.
71. Krashes MJ, et al. (2009) A neural circuit mechanism integrating motivational state with memory expression in *Drosophila*. *Cell* 139:416–427.
72. Perisse E, et al. (2013) Different Kenyon cell populations drive learned approach and avoidance in *Drosophila*. *Neuron* 79:945–956.
73. Thum AS, Jenett A, Ito K, Heisenberg M, Tanimoto H (2007) Multiple memory traces for olfactory reward learning in *Drosophila*. *J Neurosci* 27:11132–11138.
74. Tully T, Quinn WG (1985) Classical conditioning and retention in normal and mutant *Drosophila melanogaster*. *J Comp Physiol A* 157:263–277.
75. Shafer OT, et al. (2008) Widespread receptivity to neuropeptide PDF throughout the neuronal circadian clock network of *Drosophila* revealed by real-time cyclic AMP imaging. *Neuron* 58:223–237.
76. Nikolaev VO, Bünemann M, Hein L, Hannawacker A, Lohse MJ (2004) Novel single chain cAMP sensors for receptor-induced signal propagation. *J Biol Chem* 279: 37215–37218.
77. Byers D, Davis RL, Kiger JA, Jr (1981) Defect in cyclic AMP phosphodiesterase due to the dunce mutation of learning in *Drosophila melanogaster*. *Nature* 289:79–81.
78. Dudaí Y, Uzzan A, Zvi S (1983) Abnormal activity of adenylate cyclase in the *Drosophila* memory mutant rutabaga. *Neurosci Lett* 42:207–212.
79. Davis RL (2005) Olfactory memory formation in *Drosophila*: From molecular to systems neuroscience. *Annu Rev Neurosci* 28:275–302.
80. Luo SX, Axel R, Abbott LF (2010) Generating sparse and selective third-order responses in the olfactory system of the fly. *Proc Natl Acad Sci USA* 107:10713–10718.
81. Han JH, et al. (2007) Neuronal competition and selection during memory formation. *Science* 316:457–460.
82. Yiu AP, et al. (2014) Neurons are recruited to a memory trace based on relative neuronal excitability immediately before training. *Neuron* 83:722–735.
83. Knudsen EI (2007) Fundamental components of attention. *Annu Rev Neurosci* 30: 57–78.
84. Zhang K, Guo JZ, Peng Y, Xi W, Guo A (2007) Dopamine-mushroom body circuit regulates saliency-based decision-making in *Drosophila*. *Science* 316:1901–1904.
85. Mao Z, Davis RL (2009) Eight different types of dopaminergic neurons innervate the *Drosophila* mushroom body neuropil: Anatomical and physiological heterogeneity. *Front Neural Circuits* 3:5.
86. Tomchik SM (2013) Dopaminergic neurons encode a distributed, asymmetric representation of temperature in *Drosophila*. *J Neurosci* 33:2166–2176.
87. Berry JA, Cervantes-Sandoval I, Chakraborty M, Davis RL (2015) Sleep facilitates memory by blocking dopamine neuron-mediated forgetting. *Cell* 161:1656–1667.
88. Szyszka P, Galkin A, Menzel R (2008) Associative and non-associative plasticity in Kenyon cells of the honeybee mushroom body. *Front Syst Neurosci* 2:3.
89. Johansen JP, et al. (2014) Hebbian and neuromodulatory mechanisms interact to trigger associative memory formation. *Proc Natl Acad Sci USA* 111:E5584–E5592.
90. Krashes MJ, Waddell S (2008) Rapid consolidation to a radish and protein synthesis-dependent long-term memory after single-session appetitive olfactory conditioning in *Drosophila*. *J Neurosci* 28:3103–3113.
91. Perisse E, et al. (2009) Early calcium increase triggers the formation of olfactory long-term memory in honeybees. *BMC Biol* 7:30.
92. Masek P, Worden K, Aso Y, Rubin GM, Keene AC (2015) A dopamine-modulated neural circuit regulating aversive taste memory in *Drosophila*. *Curr Biol* 25: 1535–1541.
93. Kaun KR, Azanchi R, Maung Z, Hirsh J, Heberlein U (2011) A *Drosophila* model for alcohol reward. *Nat Neurosci* 14:612–619.
94. Owald D, Waddell S (2015) Olfactory learning skews mushroom body output pathways to steer behavioral choice in *Drosophila*. *Curr Opin Neurobiol* 35:178–184.
95. Joiner WJ, Crocker A, White BH, Sehgal A (2006) Sleep in *Drosophila* is regulated by adult mushroom bodies. *Nature* 441:757–760.
96. Pitman JL, McGill JJ, Keegan KP, Allada R (2006) A dynamic role for the mushroom bodies in promoting sleep in *Drosophila*. *Nature* 441:753–756.
97. Sitaraman D, et al. (2015) Propagation of homeostatic sleep signals by segregated synaptic microcircuits of the *Drosophila* mushroom body. *Curr Biol* 25:2915–2927.
98. Acevedo SF, Froudarakis EI, Kanellopoulos A, Skoulakis EM (2007) Protection from premature habituation requires functional mushroom bodies in *Drosophila*. *Learn Mem* 14:376–384.
99. Bang S, et al. (2011) Dopamine signalling in mushroom bodies regulates temperature-preference behaviour in *Drosophila*. *PLoS Genet* 7:e1001346.
100. Pfeiffer BD, et al. (2010) Refinement of tools for targeted gene expression in *Drosophila*. *Genetics* 186:735–755.